Electronic Supplementary Material (ESI) for Environmental Science: Nano.

Electronic Supporting Information

Synergetic Effect of Physicochemical and Electrostatic Strategies on Ion Sieving for Polymer Cross-linked Graphene Oxide Membrane

Ki Ryuk Bang,[a] Daniel Bahamon,[b,c] Lourdes F. Vega*[b,c] and Eun Seon Cho*[a]

[a] Department of Chemical and Biomolecular Engineering, Korea Advanced Institute of Science and Technology (KAIST), Daejeon 34141, Republic of Korea

[b] Research and Innovation Center on CO_2 and Hydrogen (RICH), and Catalysis and Separation Center (CeCaS). Khalifa University, PO Box 127788, Abu Dhabi, UAE

[c] Chemical Engineering Department, Khalifa University, PO Box 127788, Abu Dhabi, UAE

* Corresponding author: escho@kaist.ac.kr; lourdes.vega@ku.ac.ae

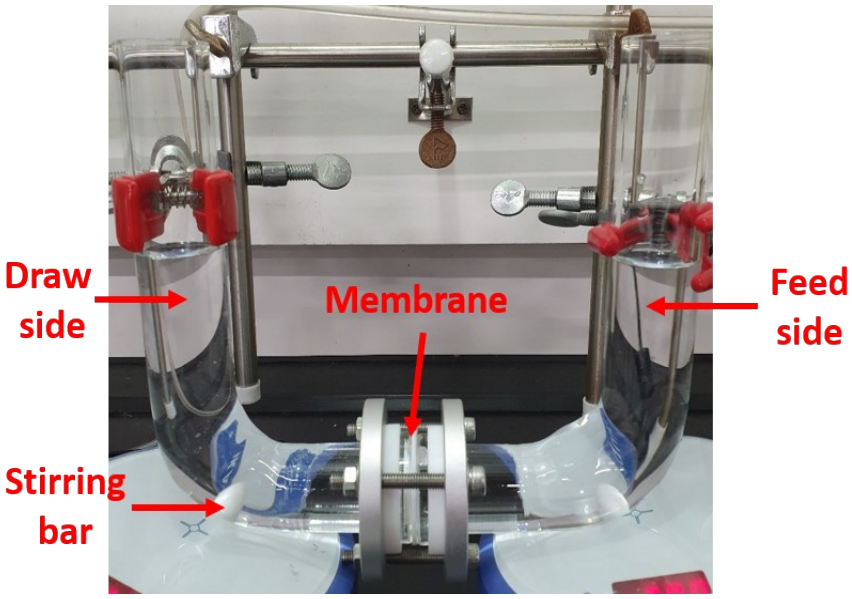

Fig. S1 A photo of homemade U-shape permeation test setup

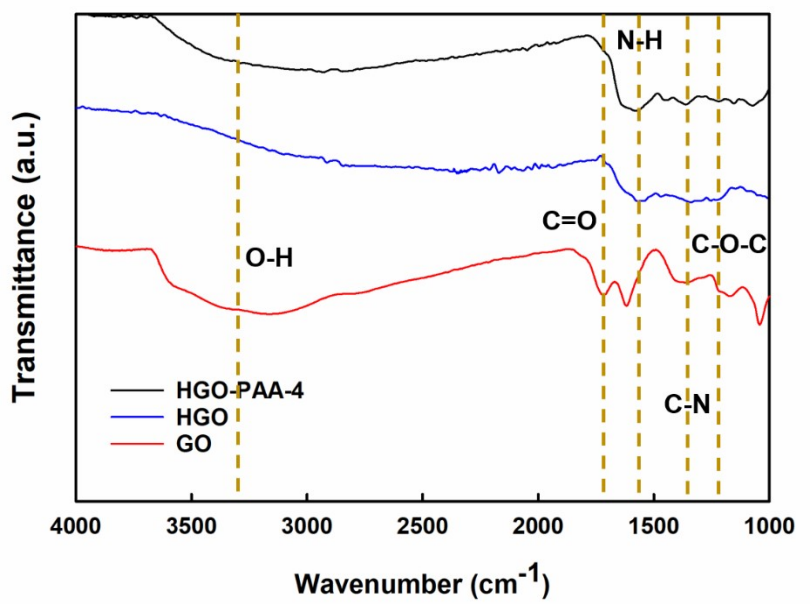

Fig. S2 FT-IR spectra of GO (red), HGO (blue) and HGO-PAA-4, respectively.

In the HGO membrane, it is found that the peak of oxygen functional groups present in the GO membrane disappear and the newly created N-H peak (1560 cm^{-1}) and C-N peak (1350 cm^{-1}) indicate the chemical reaction between GO and HPEI polymer successfully proceeds.[1-3] After treatment of the PAA polymer into the HGO membrane, the carboxylic acid peak (1710 cm^{-1}) slightly appears again in the HGO-PAA membrane[3] and the characteristic C-N peak is intensified, indicating that not only is the PAA polymer well inserted into the composite membrane system, but the covalent bond is freshly formed between two polymers. In addition, the imide peak (1733 cm^{-1}) of the urea by-product is not shown in the spectra of the HGO-PAA-4 due to the thorough washing process.[4,5]

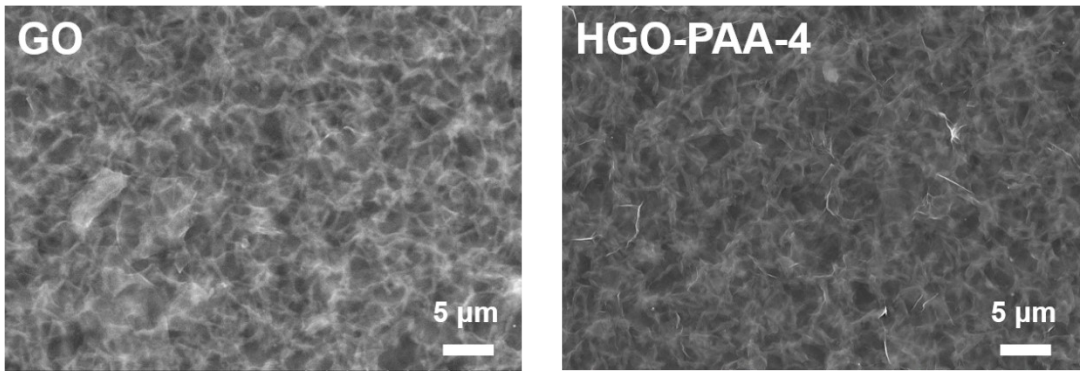

Fig. S3 Top-down SEM images of the GO and HGO-PAA-4 membrane

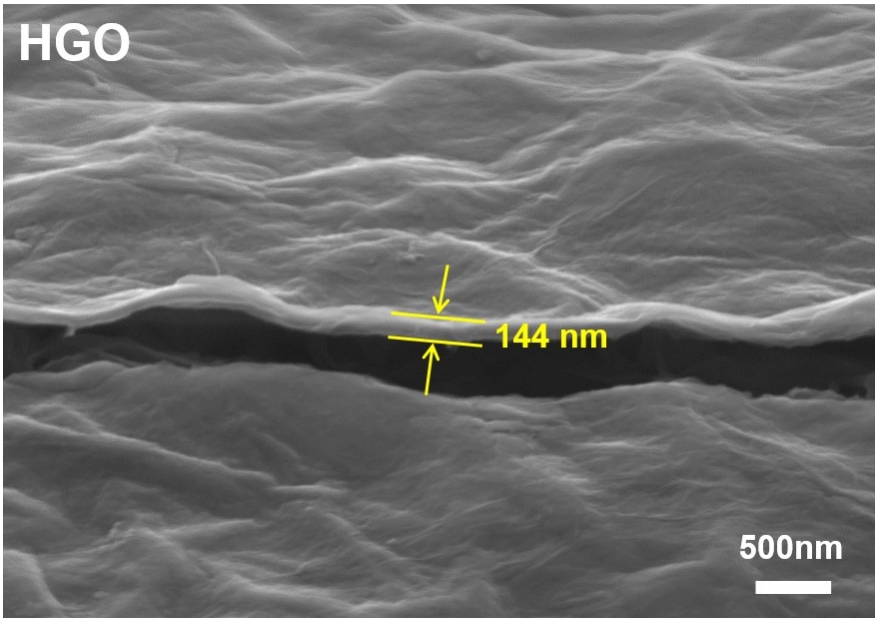

Fig. S4 Cross-sectional SEM image of the HGO membrane

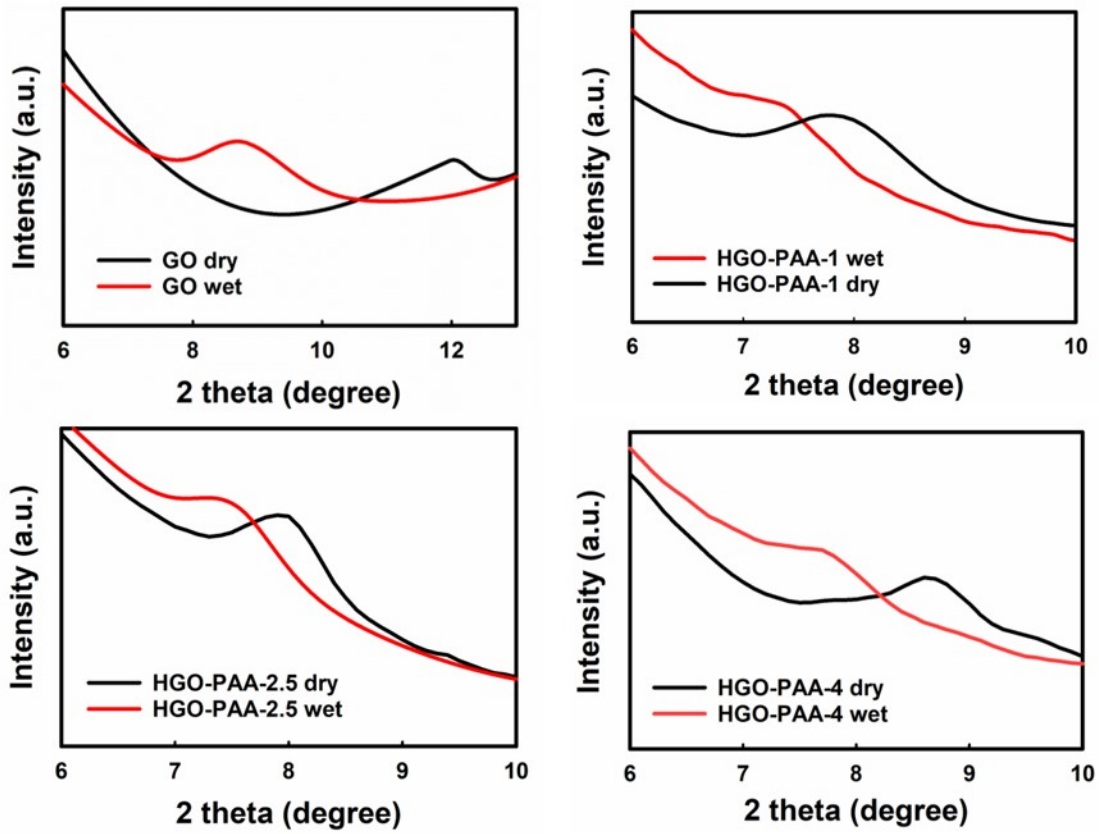

Fig. S5 XRD spectra of the GO and HGO-PAA composite membranes in dry and in wet state.

To figure out the channel size of composite membranes in wet state, the GO composite membranes are treated by DI water. DI water is dropped on the surface of the composite membrane for 5 min to eliminate the swelling effect of the polymer substrate.

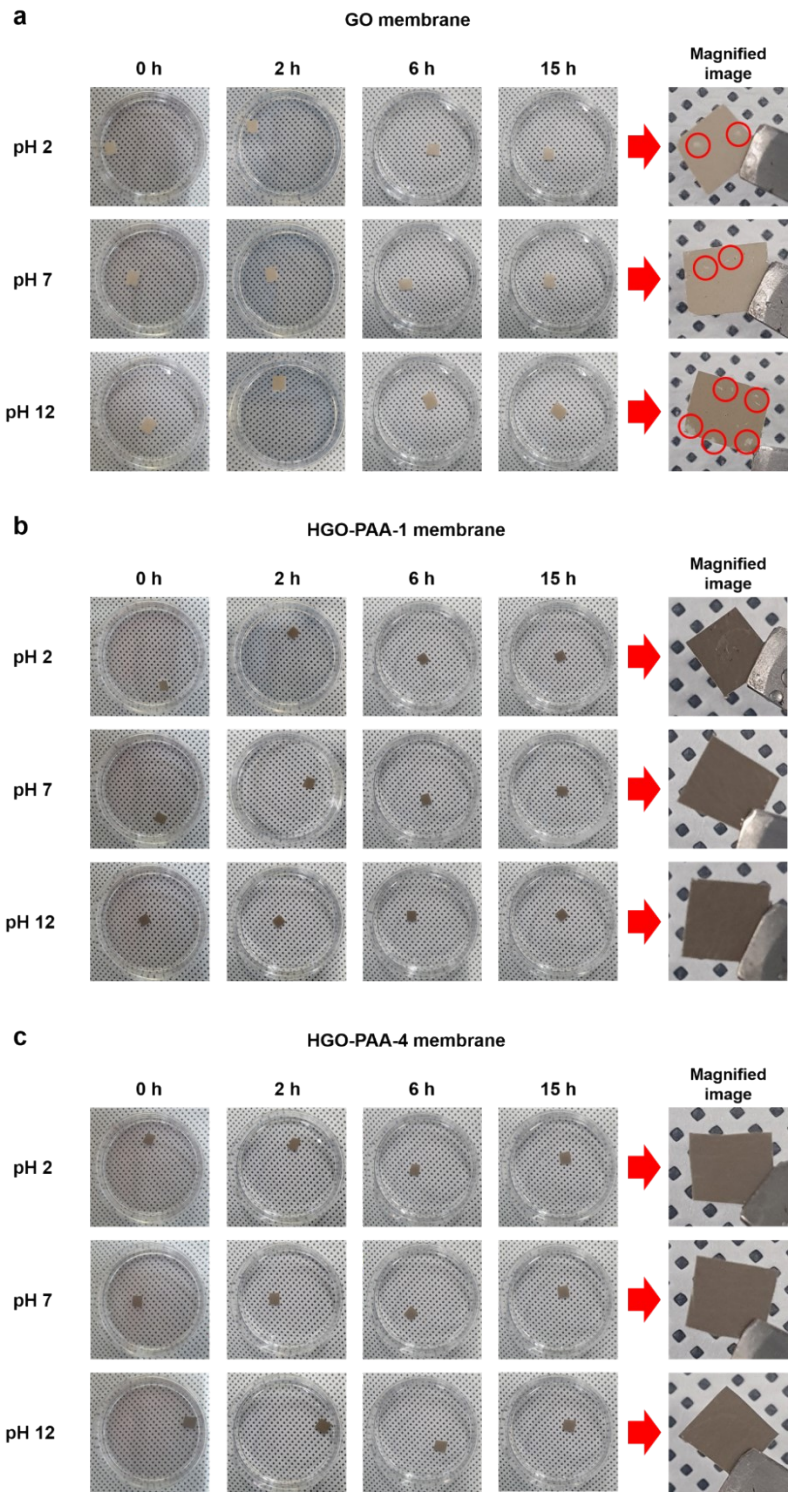

Fig. S6 Membrane stability test of (a) the GO membrane (the red-circles show that some parts of the membrane have been peeled off.), (b) HGO-PAA-1 and (c) HGO-PAA-4 membrane in different pH conditions.

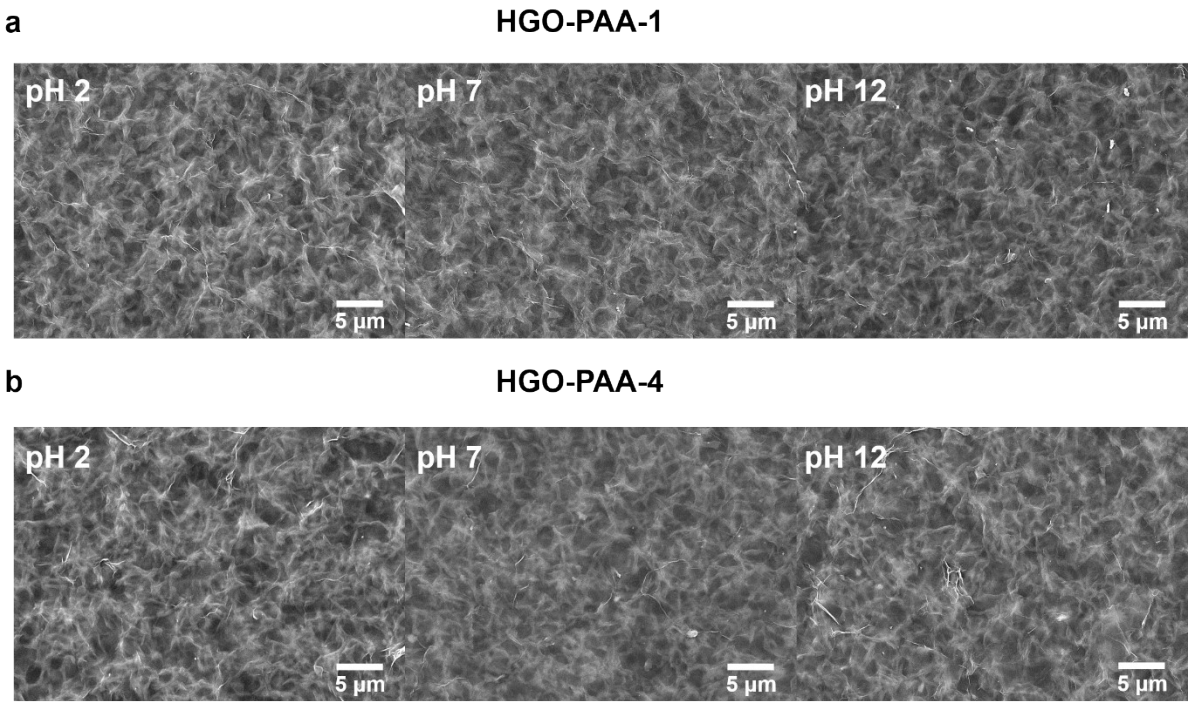

Fig. S7 Top-down SEM images of (a) HGO-PAA-1 and (b) HGO-PAA-4 membrane after membrane stability tests in different pH conditions.

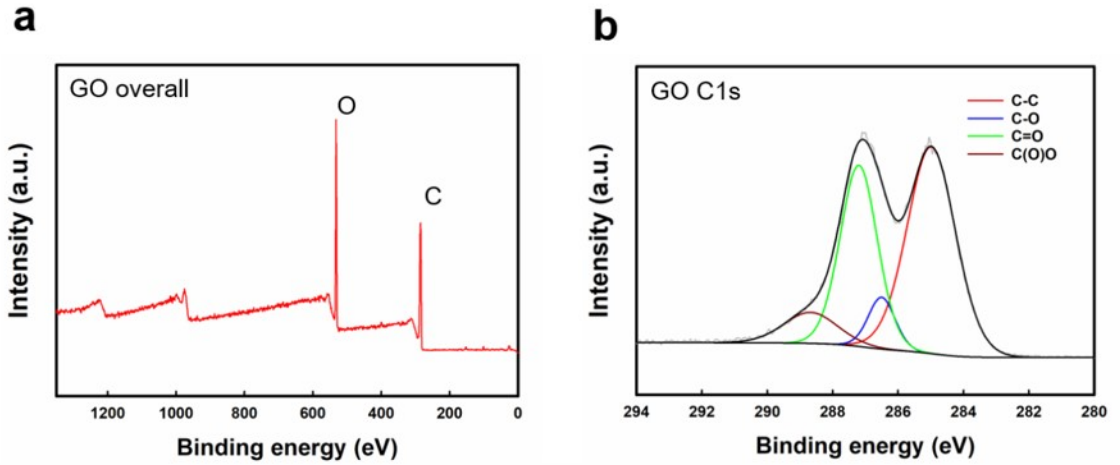

Fig. S8 (a) Overall scan, (b) C1s XPS spectra of the pristine GO membrane

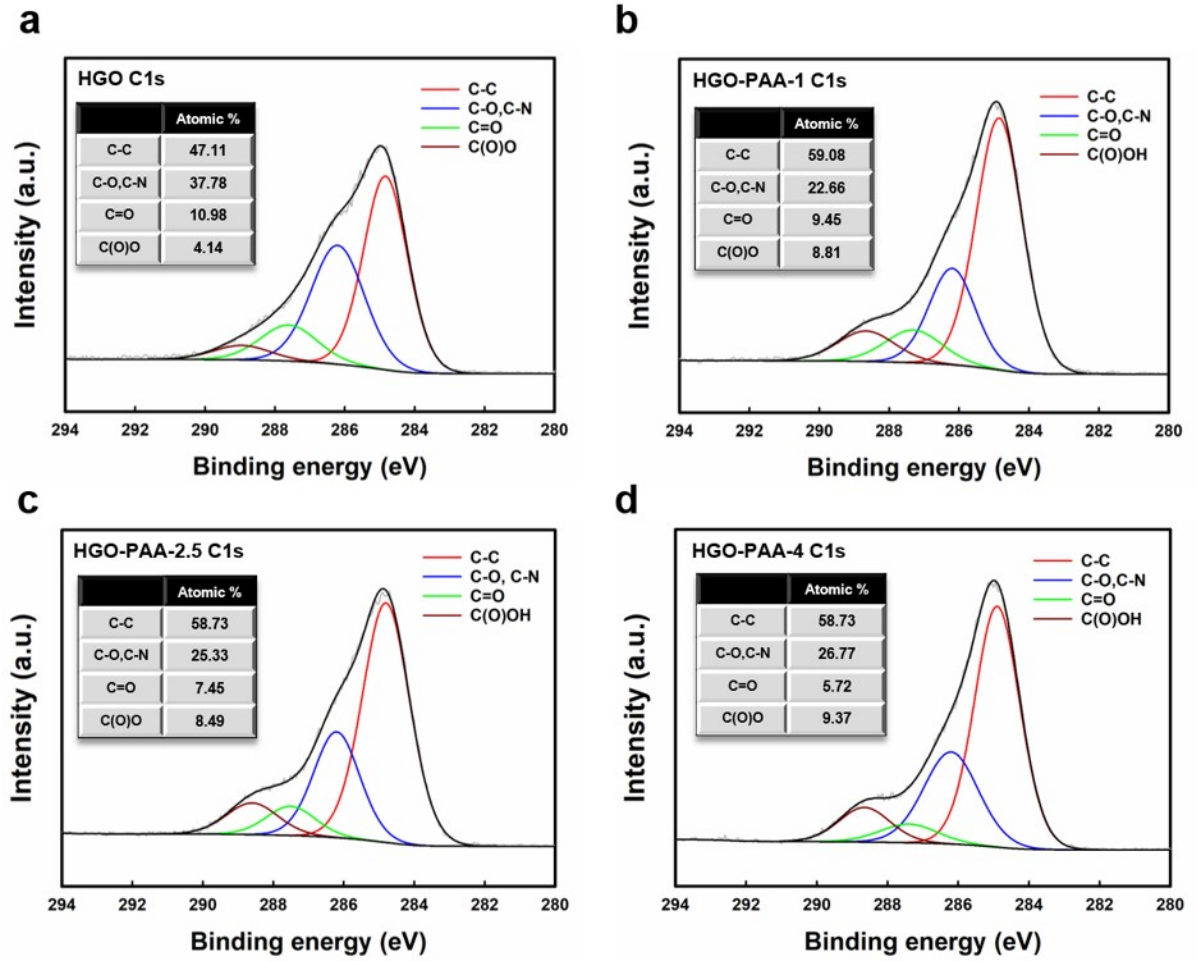

Fig. S9 XPS analysis for chemical composition of HGO and HGO-PAA composite membranes. C1s XPS spectra with the deconvolution results for (a) HGO, (b) HGO-PAA-1, (c) HGO-PAA-2.5 and (d) HGO-PAA-4, respectively.

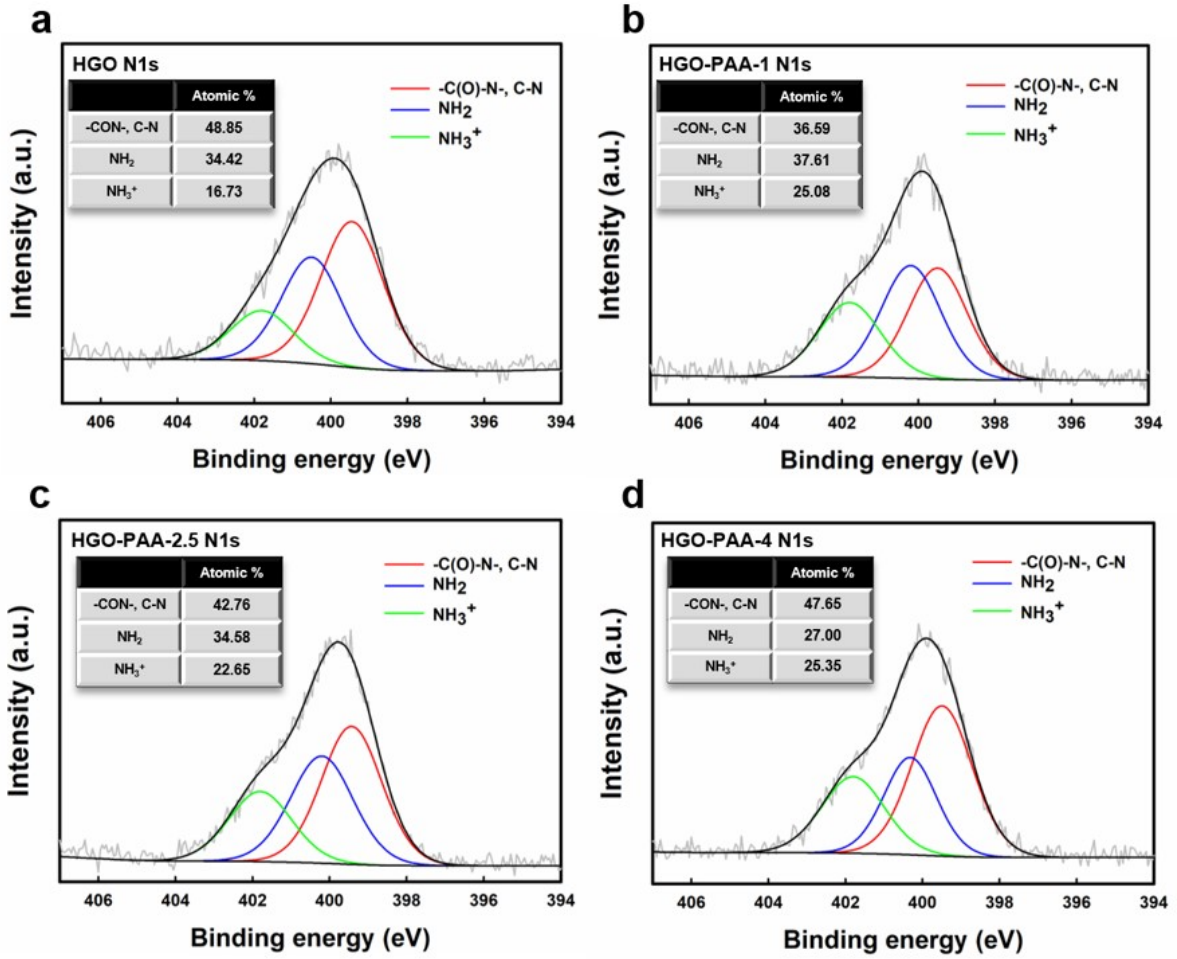

Fig. S10 N1s XPS spectra with the deconvolution results for (a) HGO, (b) HGO-PAA-1, (c) HGO-PAA-2.5 and (d) HGO-PAA-4, respectively.

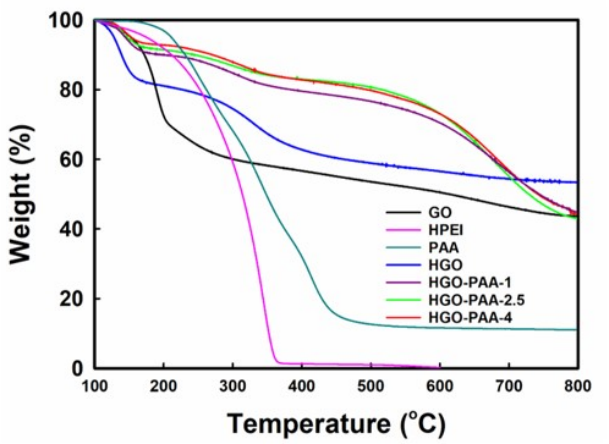

	Percentage of inserted PAA in the composite membrane
1 bar	19.9 %
2.5 bar	24.0 %
4 bar	21.1 %

Fig. S11 Thermogravimetric analysis (TGA) curve of the GO, HGO and HGO-PAA membranes, and the percentage of inserted PAA in the composite membrane depending on the applied pressure.

The PAA percentage inserted into the HGO-PAA membrane can be calculated from TGA curves. When the temperature is raised to 800 ˚C, the remaining weight percentage of the HGO membrane is 53.3%, and the residue of pure PAA is about 11 %. The weight of the HGO-PAA-1 is 0.602 mg at 100 ˚C. After heating to 800 ˚C, the weight of the residue is 0.270 mg. Based on this result, since the thermal decomposition of both the HGO structure and the PAA structure could occur at 800 ˚C except for the influence of bond breakage, it can be concluded that 53.3 % of HGO and 11 % of PAA remain in the residue. If the equation is solved based on this result, the PAA composition of each HGO-PAA-1, HGO-PAA-2.5 and HGO-PAA-4 is 19.9 %, 24.0 %, and 21.1%, respectively. Therefore, it can be confirmed that a similar amount of PAA is intercalated into the HGO membrane regardless of the applied pressure.

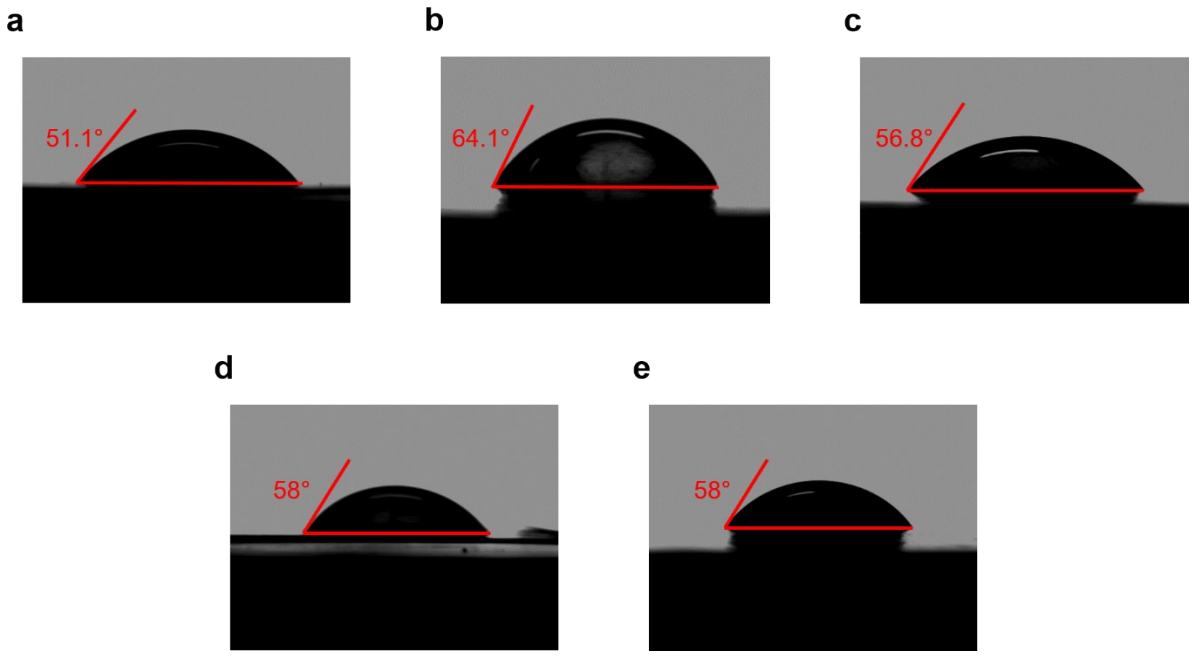

Fig. S12 Water contact angle of (a) the neat GO membrane, (b) HGO membrane, (c) HGO-PAA-1, (d) HGO-PAA-2.5, and (e) HGO-PAA-4 membrane.

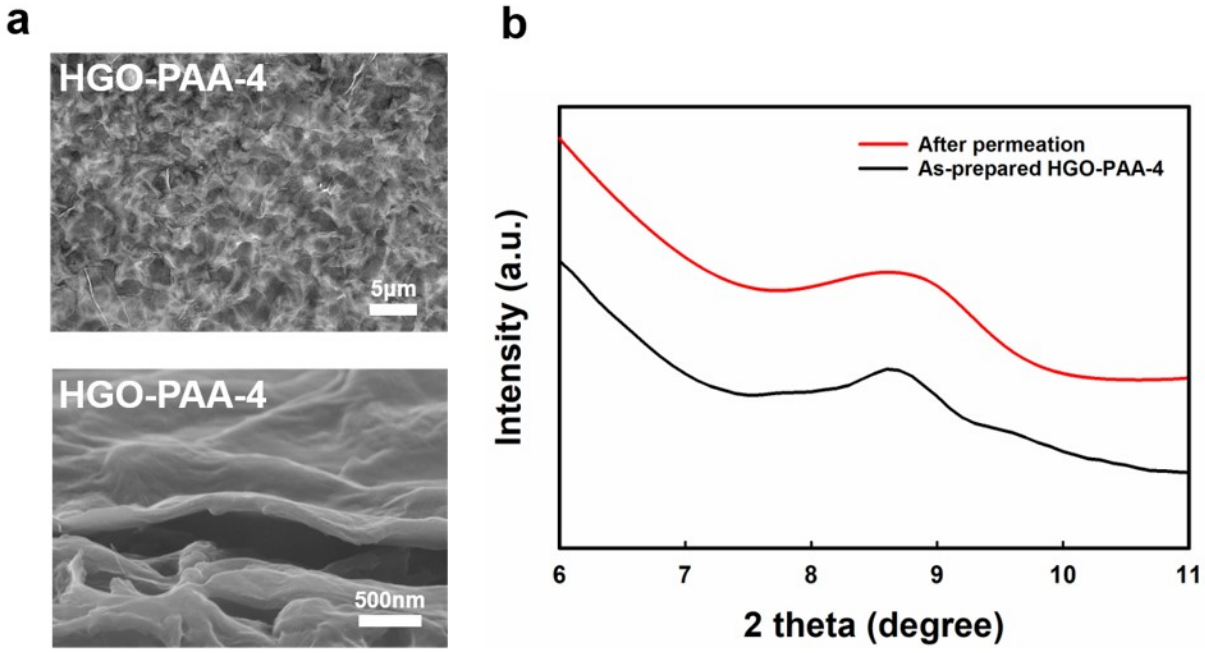

Fig. S13 (a) Top-down and cross-sectional SEM images of the HGO-PAA-4 after the NaCl permeation test. (b) XRD spectra of the as-prepared HGO-PAA-4 and HGO-PAA-4 after the permeation test.

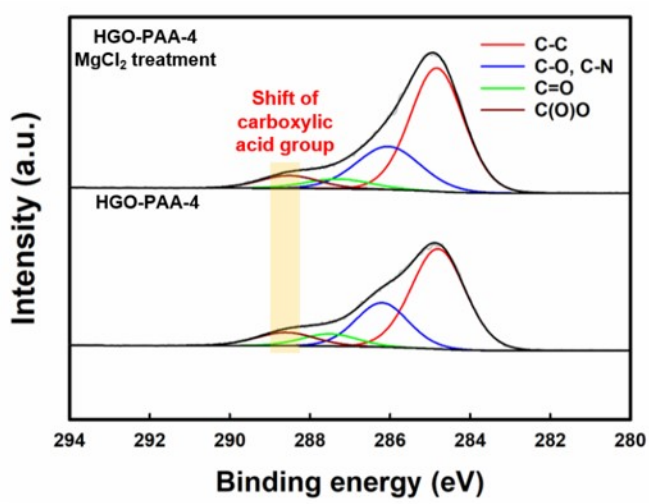

Fig. S14 C1s XPS spectra of the HGO-PAA-4 with and without Mg ions.

The carboxylic acid groups of PAA in the HGO-PAA-4 could form chelating structure with ionic species. A slight peak shift of carboxylic acid groups from 288.6 eV to 288.45 eV indicates that electrostatic attraction forces between the functional groups and Mg ions can be generated, which is similar to the previous result with respect to the interaction between metal ions and carboxylate groups.[6-8]

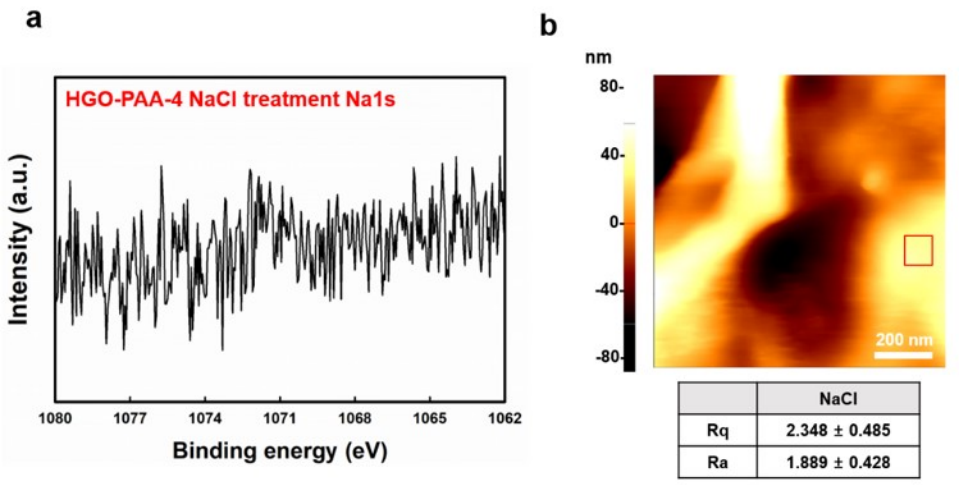

Fig. S15 (a) Na 1s XPS spectra of the HGO-PAA-4 treated with NaCl. (b) AFM scan images of the HGO-PAA-4 membrane treated by NaCl. Rq and Ra values were obtained by the measurement at 5 spots which have similar brightness from the scan image (scan size 1 μm x 1 μm).

a

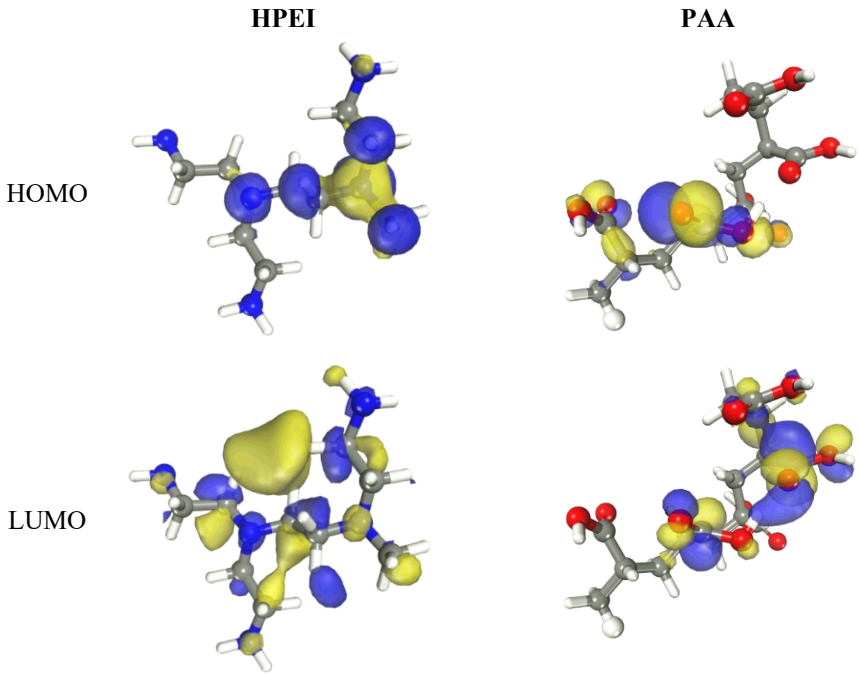

b

	E_{HOMO} (eV)		E_{LUMO} (eV)		ΔE_{gap} (eV)	
	Vacuum	**Aqueous ("wet")**	**Vacuum**	**Aqueous ("wet")**	**Vacuum**	**Aqueous ("wet")**
HPEI	-3.99	-4.14	+1.27	+0.97	-5.26	-5.11
PAA	-5.73	-6.26	-0.99	-1.61	-4.74	-4.65

Fig. S16 (a) HOMO and LUMO charge distributions for representations of HPEI and PAA polymers studied using the implicit solvation model (blue regions for electron accumulation and yellow regions for electron loss); (b) bandgap energies for the optimized structures of the polymers in both vacuum and aqueous phase (color code: gray for carbon atoms, blue for nitrogen atoms, red for oxygen atoms, white for hydrogen atoms).

In addition to MD, density functional theory (DFT) calculations of studied polymers were performed to evaluate the chemical reactivity and chemical group interactions (Figure S16), in both vacuum and in implicit water solvation conditions. The implicit water solvation, despite its

simplicity, provides a more adequate estimate of the electron donation and acceptance ability than the vacuum calculations.[9,10] It was found that the HOMO (Highest Occupied Molecular Orbital) and LUMO (Lowest Unoccupied Molecular Orbital) electron densities of HPEI and PAA are distributed along the amine and carboxylic groups, respectively, with weak charge localization near the edges, indicating that the excess electrons can be donated. This reveals the theoretical electron donation and acceptance ability of the composite membrane in aqueous solutions. In addition, the high E_{HOMO} values are an indication of an ease flow of electrons to p-orbitals of the GO surface. Lower (more negative) band gap energy (ΔE_{gap}) of HPEI results in higher reactivity of the polymeric molecule, potentially leading to easier adsorption on the GO surface.

Table S1. Zeta-potential of the neat GO, HGO and HGO-PAA membranes in DI water.

Membrane	Zeta-potential (mV)
GO	-54.0 ± 8.96
HGO	-27.6 ± 4.61
HGO-PAA-1	-45.6 ± 5.47
HGO-PAA-2.5	-41.3 ± 6.05
HGO-PAA-4	-43.6 ± 8.91

Table S2. Performance comparisons of synthesized HGO-PAA membranes with other membranes

Membrane	Method	Thickness	Feed concentration	Diffusion rate ($mol \cdot m^{-2} h^{-1}$) / Rejection rate (%)	Water flux ($L \cdot m^{-2} h^{-1}$)	Reference
Untreated GO-280	Diffusion	280 nm	0.25 M	0.718 (Na^+ only)	0.85	11
KCl-controlled GO-280	Diffusion	280 nm	0.25 M	0.0048 (Na^+ only)	0.36	11
Ca-SAT membrane	Diffusion	3 μm	0.5 M	0.4 (NaCl)	X	12
HG crosslinked GO	Diffusion	17.1 μm	0.05 M	0.024 (KCl)	X	13
GO/LDH-NS (Co-Al)	Diffusion	3.2 μm	0.1 M	~0.16 (NaCl)	X	14
MXene	Diffusion	1.5 μm	0.2 M	1.53 (Na^+ only)	X	15
PEI/GO/h-PAN	Dead-end filtration	59.1 nm	1000 ppm	38.1 % (NaCl)	4.2 (LMH/bar) at 5 bar	16
GO&EDA_H PEI 60K	Dead-end filtration	69.4 nm	1000 ppm	~55 % (NaCl)	5 (LMH/bar) at 1 bar	17
GO-PAA	Dead-end filtration	125 nm	50 ppm	95.3 % (Na_2SO_4)	14.3 (LMH/bar) at 2 bar	18
Pristine GO	Diffusion	~140 nm	0.25 M	1.095 (NaCl)	2.43	This work
HGO-PAA-4	Diffusion	~140 nm	0.25 M	0.227 (NaCl)	3.98	This work

Table S3. Comparison of interlayer distance (*d*-spacing between GO sheets) calculated with MD simulations and measured experimentally for different evaluated systems.

	GO	**HGO-PAA-1**	**HGO-PAA-2.5**	**HGO-PAA-4**
Wet (EXP)	9.98 Å	12.08 Å	11.90 Å	11.28 Å
Wet (SIM)	10.8 Å	11.9 Å	---	11.6 Å

Since GO layers are not completely flat due to interactions with both water and polymers, there are regions in which GO sheets are separated by a different number of water layers. Therefore, the *d*-spacing was calculated in the MD simulations as the average distance between the upper sheet and the lower sheet. Moreover, the water molecules in the nano-sized capillaries of GO membranes cause swelling, hence, such distance was controlled by applying an external force to the system (in a similar manner as in the experimental section).

REFERENCES

1. B. Xue, J. Zhu, N. Liu and Y. Li, Facile functionalization of graphene oxide with ethylenediamine as a solid base catalyst for Knoevenagel condensation reaction, *Catal. Commun.*, 2015, **64**, 105-109.
2. H. Liu, T. Kuila, N. H. Kim, B.-C. Ku and J. H. Lee, In situ synthesis of the reduced graphene oxide–polyethyleneimine composite and its gas barrier properties, *J. Mater. Chem. A*, 2013, **1**.
3. W.-S. Hung, C.-H. Tsou, M. De Guzman, Q.-F. An, Y.-L. Liu, Y.-M. Zhang, C.-C. Hu, K.-R. Lee and J.-Y. Lai, Cross-Linking with Diamine Monomers To Prepare Composite Graphene Oxide-Framework Membranes with Varying d-Spacing, *Chem. Mater.*, 2014, **26**, 2983-2990.
4. C. Wang, Q. Yan, H. B. Liu, X. H. Zhou and S. J. Xiao, Different EDC/NHS activation mechanisms between PAA and PMAA brushes and the following amidation reactions, *Langmuir*, 2011, **27**, 12058-12068.
5. J. R. Dunetz, J. Magano and G. A. Weisenburger, Large-Scale Applications of Amide Coupling Reagents for the Synthesis of Pharmaceuticals, *Org. Process Res. Dev.*, 2016, **20**, 140-177.
6. M. Rosillo-Lopez and C. G. Salzmann, Highly efficient heavy-metal extraction from water with carboxylated graphene nanoflakes, *RSC Adv.*, 2018, **8**, 11043-11050.
7. R. Sitko, E. Turek, B. Zawisza, E. Malicka, E. Talik, J. Heimann, A. Gagor, B. Feist and R. Wrzalik, Adsorption of divalent metal ions from aqueous solutions using graphene oxide, *Dalton Trans.*, 2013, **42**, 5682-5689.

8. S. Park, K. S. Lee, G. Bozoklu, W. Cai, S. T. Nguyen and R. S. Ruoff', Graphene oxide papers modified by divalent ions - Enhancing mechanical properties via chemical cross-linking, *ACS Nano*, 2008, **2**, 572-578.

9. E. Aquino-Torres, R. L. Camacho-Mendoza, E. Gutierrez, J. A. Rodriguez, L. Feria, P. Thangarasu and J. Cruz-Borbolla, The influence of iodide in corrosion inhibition by organic compounds on carbon steel: Theoretical and experimental studies, *Appl. Surf. Sci.*, 2020, **514**.

10. R. Aslam, M. Mobin, J. Aslam and H. Lgaz, Sugar based N,N'-didodecyl-N,N'digluconamideethylenediamine gemini surfactant as corrosion inhibitor for mild steel in 3.5% NaCl solution-effect of synergistic KI additive, *Sci. Rep.*, 2018, **8**, 3690.

11. L. Chen, G. Shi, J. Shen, B. Peng, B. Zhang, Y. Wang, F. Bian, J. Wang, D. Li, Z. Qian, G. Xu, G. Liu, J. Zeng, L. Zhang, Y. Yang, G. Zhou, M. Wu, W. Jin, J. Li and H. Fang, Ion sieving in graphene oxide membranes via cationic control of interlayer spacing, *Nature*, 2017, **550**, 380-383.

12. J. Wang, Z. Zhang, J. Zhu, M. Tian, S. Zheng, F. Wang, X. Wang and L. Wang, Ion sieving by a two-dimensional Ti3C2Tx alginate lamellar membrane with stable interlayer spacing, *Nat. Commun.*, 2020, **11**, 3540.

13. Z. Jia and Y. Wang, Covalently crosslinked graphene oxide membranes by esterification reactions for ions separation, *J. Mater. Chem. A*, 2015, **3**, 4405-4412.

14. P. Sun, R. Ma, W. Ma, J. Wu, K. Wang, T. Sasaki and H. Zhu, Highly selective charge-guided ion transport through a hybrid membrane consisting of anionic graphene oxide and cationic hydroxide nanosheet superlattice units, *NPG Asia Mater.*, 2016, **8**, e259-e259.

15. C. E. Ren, K. B. Hatzell, M. Alhabeb, Z. Ling, K. A. Mahmoud and Y. Gogotsi, Charge- and Size-Selective Ion Sieving Through Ti3C2Tx MXene Membranes, *J. Phys. Chem. Lett.*, 2015, **6**, 4026-4031.

16. Q. Nan, P. Li and B. Cao, Fabrication of positively charged nanofiltration membrane via the layer-by-layer assembly of graphene oxide and polyethylenimine for desalination, *Appl. Surf. Sci.*, 2016, **387**, 521–528.

17. Y. Zhang, S. Zhang and T.-S. Chung, Nanometric Graphene Oxide Framework Membranes with Enhanced Heavy Metal Removal via Nanofiltration, *Environ. Sci. Technol.*, 2015, **49**, 10235–10242.

18. M. Zhang, K. Guan, Y. Ji, G. Liu, W. Jin and N. Xu, Controllable ion transport by surface-charged graphene oxide membrane, *Nat. Commun.*, 2019, **10**, 1253.